Crystal structure and Hirshfeld surface analysis of (Z)-4-({[2-(benzo[b]thiophen-3-yl)cyclopent-1-en-1-yl]methyl}(phenyl)amino)-4-oxobut-2-enoic acid

Elizaveta D. Yakovleva,[a] Evgeniya R. Shelukho,[a] Mikhail S. Grigoriev,[b] Khudayar I. Hasanov,[c,d] Nurlana D. Sadikhova,[e] Mehmet Akkurt[f] and Ajaya Bhattarai[g]*

[a]RUDN University, 6 Miklukho-Maklaya St., Moscow 117198, Russian Federation, [b]Frumkin Institute of Physical Chemistry and Electrochemistry, Russian Academy of Sciences, Leninskiy prospect 31-4, Moscow 119071, Russian Federation, [c]Western Caspian University, Istiqlaliyyat Street 31, AZ 1001, Baku, Azerbaijan, [d]Azerbaijan Medical University, Scientific Research Centre (SRC), A. Kasumzade St. 14, AZ 1022, Baku, Azerbaijan, [e]Department of Chemistry, Baku State University, Z. Xalilov Str. 23, AZ 1148 Baku, Azerbaijan, [f]Department of Physics, Faculty of Sciences, Erciyes University, 38039 Kayseri, Türkiye, and [g]Department of Chemistry, M.M.A.M.C. (Tribhuvan University), Biratnagar, Nepal. *Correspondence e-mail: ajaya.bhattarai@mmamc.tu.edu.np

In the title compound, $C_{24}H_{21}NO_3S$, the cyclopentene ring adopts an envelope conformation. In the crystal, molecules are linked by C—H···π interactions, forming ribbons along the a axis. Intermolecular C—H···O hydrogen bonds connect these ribbons to each other, forming layers parallel to the ($0\bar{1}1$) plane. The molecular packing is strengthened by van der Waals interactions between the layers. The intermolecular contacts were quantified using Hirshfeld surface analysis and two-dimensional fingerprint plots, revealing the relative contributions of the contacts to the crystal packing to be H···H 46.0%, C···H/H···C 21.1%, O···H/H···O 20.6% and S···H/H···S 9.0%.

1. Chemical context

Of particular practical value in chemistry are multicomponent approaches based on cycloaddition reactions, which make it possible to selectively increase the functional periphery around a heterocyclic scaffold in two to four simple steps while achieving high structural and stereochemical diversity of the products. At the same time, of additional interest is the strategy of the method for preparing heterocyclic assemblies based on the intramolecular cyclocondensation of 3-(hetaryl)-allylamines under the action of unsaturated acid anhydrides – the IMDAV reaction (the IntraMolecular Diels–Alder reaction in Vinylarenes) (Krishna *et al.*, 2022). This work is a continuation of studies on the mechanism of the tandem acylation/[4 + 2]-cycloaddition reaction between 3-(hetaryl)-allylamines and maleic anhydride as an example of the IMDAV approach (Horak *et al.*, 2015, 2017; Nadirova *et al.*, 2020; Zubkov *et al.*, 2016; Yakovleva *et al.*, 2024). On the other hand, functionalization of amines with multiple coordination centres can be used as an important synthetic strategy for the preparation of new functional materials (Akbari Afkhami *et al.*, 2017; Abdelhamid *et al.*, 2011; Khalilov *et al.*, 2021; Safavora *et al.*, 2019). In fact, those substituents or functional groups can participate in various sorts of intermolecular interactions (Gurbanov *et al.*, 2018, 2020, 2022*a,b*; Kopylovich *et al.*, 2011*a,b,c*; Mahmudov *et al.*, 2013, 2021), which improve the function of supramolecular networks. The co-operation of weak interactions with the coordination bond in N-donating ligands can be used in the crystal engineering of tectons (Aliyeva *et al.*, 2024; Mahmoudi *et al.*, 2017*a,b*, 2019, 2021).
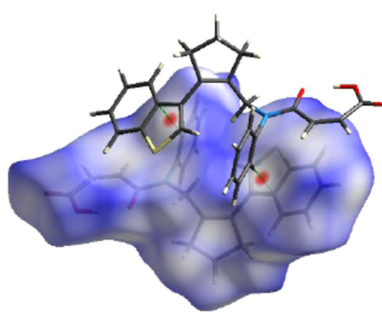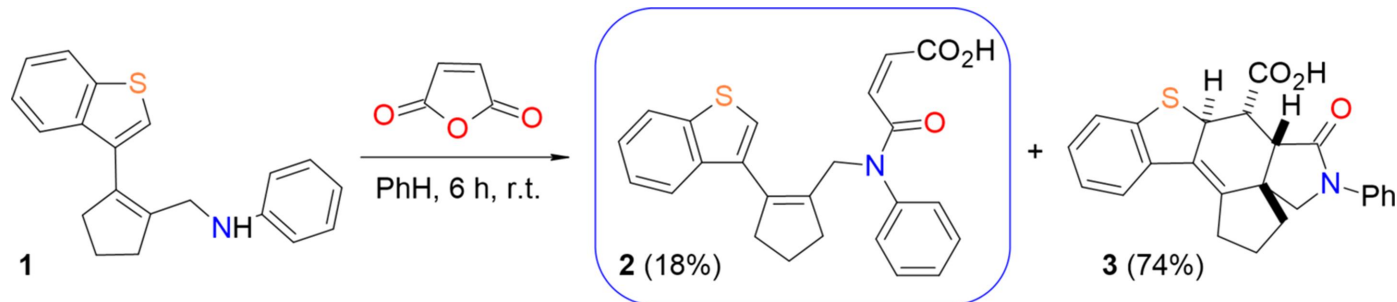
Figure 1
Synthesis of **2**.

Benzothienylallylamine **1** (Yakovleva *et al.*, 2024) is able to readily react with maleic anhydride providing a mixture of products **2** and **3** in nearly quantitative yield. The synthesis and spectral data for the major adduct **3** have been published previously (Yakovleva *et al.*, 2024), but the minor amide **2** could not be isolated and characterized because of its high tendency to spontaneously cyclize with the formation of **3** (Fig. 1). In this work, under mild reaction conditions, we successfully isolated and characterized the intermediate maleic amide **2**. Detection of amide **2** confirms directly an assumption that the IMDAV reaction begins with an acylation step followed by an intramolecular [4 + 2]-cycloaddition.

(r.m.s. deviation = 0.002 Å), while the cyclopentene ring (C11–C15) adopts an envelope conformation, with the C14 atom as the flap [puckering parameters (Cremer & Pople, 1975) are $Q(2) = 0.200\ (3)$ Å and $\varphi(2) = 103.3\ (7)°$]. The nine-membered ring system makes an angle of 66.00 (11)° with the r.m.s. plane of the cyclopentene ring. These planes make angles of 61.68 (10) and 64.83 (12)° with the phenyl ring, respectively. The C12—C11—C1—N5, C11—C1—N5—C24, C11—C1—N5—C31, N5—C24—C23—C22, O28—C24—C23—C22, C23—C22—C21—O2 and C23—C22—C21—O29 torsion angles are 117.2 (2), 102.2 (2), −80.0 (2), −177.6 (2), 3.1 (4),
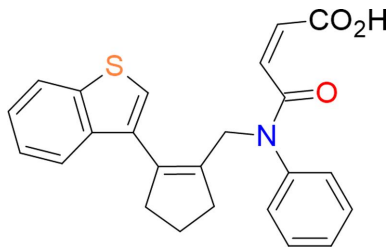
## 2. Structural commentary

As can be seen in Fig. 2, the nine-membered ring system (S1/C2/C3/C3*A*/C4-C7/C7*A*) of the molecule is essentially planar
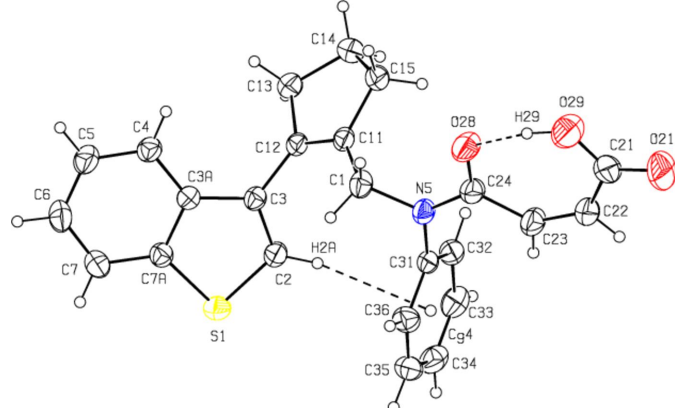

Figure 2
The molecular structure of the title compound, showing the atom labelling and displacement ellipsoids at the 30% probability level.
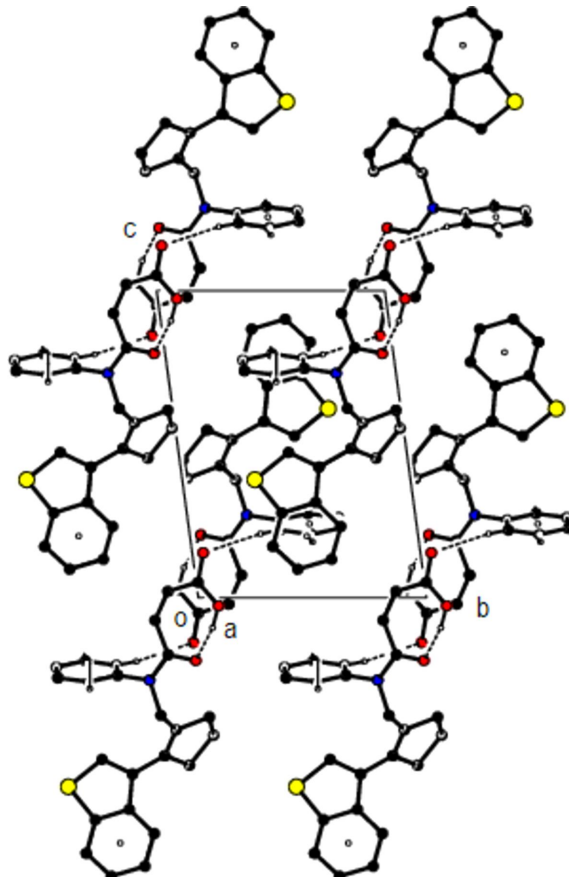
Figure 3
The crystal packing along the *a* axis, showing O—H···O, C—H···O and C—H···π interactions.
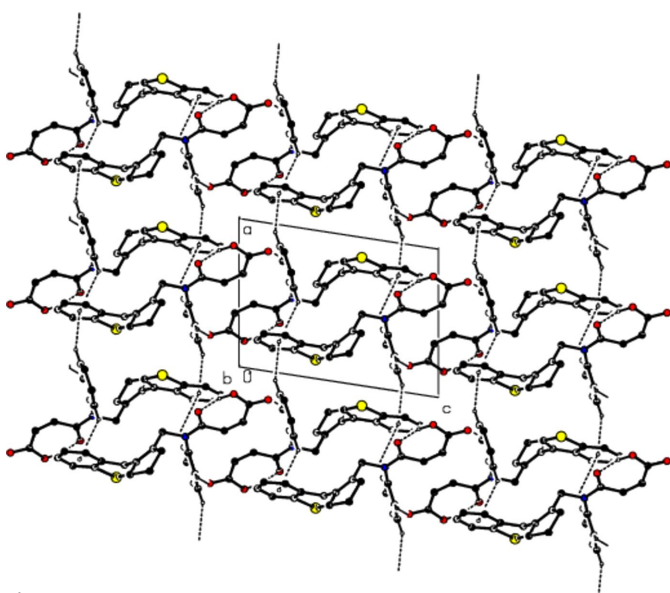
Figure 4
The crystal packing along the *b* axis, showing the O—H···O, C—H···O and C—H···π interactions.
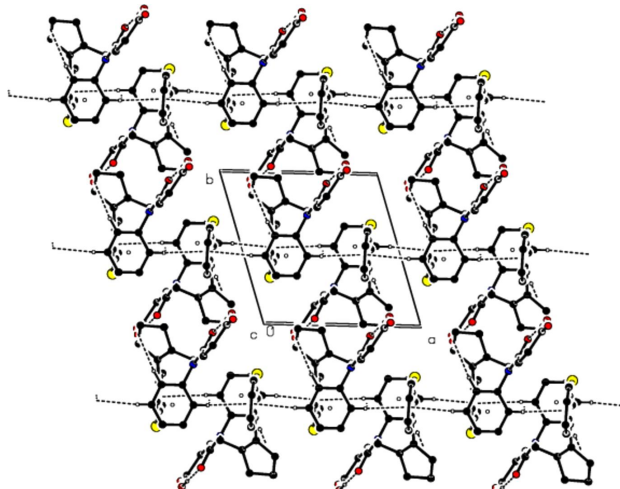
Figure 5
The crystal packing along the *c* axis, showing the O—H···O, C—H···O and C—H···π interactions.

Table 1
Hydrogen-bond geometry (Å, °).

*Cg*3 and *Cg*4 are the centroids of the benzene ring (C3*A*/C4–C7/C7*A*) of the nine-membered ring system (S1/C2-C3/C3*A*/C4–C7/C7*A*) and the phenyl ring (C31–C36), respectively.

D—H···A	D—H	H···A	D···A	D—H···A
O29—H29···O28	0.93 (4)	1.60 (4)	2.510 (3)	164 (4)
C32—H32A···O21[i]	0.93	2.63	3.556 (3)	171
C2—H2A···Cg4	0.93	2.72	3.579 (2)	154
C33—H33A···Cg3[ii]	0.93	2.54	3.408 (3)	155
C36—H36A···Cg3[iii]	0.93	2.79	3.535 (3)	138

Symmetry codes: (i) $-x+1, -y, -z$; (ii) $-x+2, -y+1, -z+1$; (iii) $-x+1, -y+1, -z+1$.

-179.9 (3) and 0.3 (5)°, respectively. The bond length and angle values of the title molecule are comparable to those of the molecules in the *Database survey* section.

3. Supramolecular features and Hirshfeld surface analysis

The molecular conformation remains stable *via* an intramolecular O29—H29···O28 hydrogen bond, which forms a ring with an *S*(7) motif, and an intramolecular C2—H2*A*··· *Cg*4 interaction (Table 1 and Fig. 2) (Bernstein *et al.*, 1995; *Cg*4 is the centroid of the C31–C36 ring). In the crystal, molecules are linked by C—H···π interactions, forming ribbons along the *a* axis. Intermolecular C—H···O hydrogen bonds connect these ribbons to each other, forming layers parallel to the (0$\bar{1}$1) plane. The molecular packing is strengthened by van der Waals interactions between the layers (Table 1 and Figs. 3, 4 and 5).

CrystalExplorer17.5 (Spackman *et al.*, 2021) was used to compute the Hirshfeld surfaces and the two-dimensional fingerprints of the title molecule. The d_{norm} mappings were performed in the range from -0.1088 (red) to $+1.5482$ (blue) a.u., on the d_{norm} surfaces, allowing the location of the C—H···O and C—H···π interactions (Table 1 and Fig. 6).

The fingerprint plots (Fig. 7) show that H···H [Fig. 7(*b*); 46.0%], C···H/H···C [Fig. 7(*c*); 21.1%], O···H/H···O

Figure 6
Front (*a*) and back (*b*) views of the three-dimensional Hirshfeld surface, with some C—H···O, O—H···O and C—H···π interactions shown.
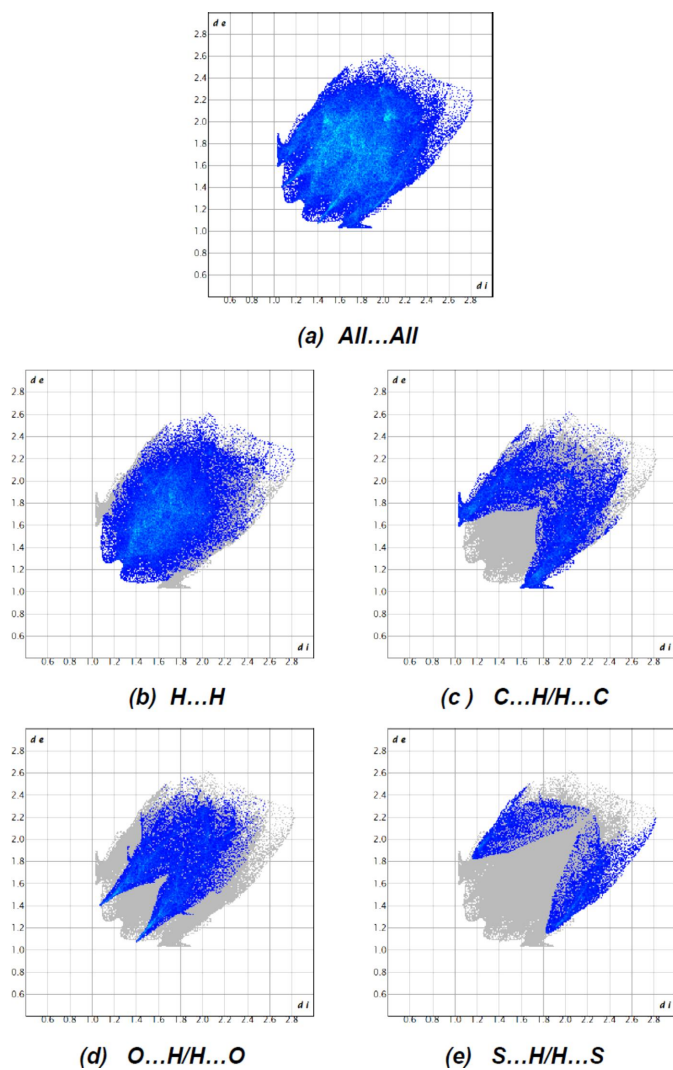
Figure 7
The two-dimensional fingerprint plots for the title molecules showing (*a*) all interactions, and delineated into (*b*) H···H, (*c*) C···H/H···C, (*d*) O···H/H···O and (*e*) S···H/H···S interactions. The d_i and d_e values are the closest internal and external distances (in Å) from given points on the Hirshfeld surface.

[Fig. 7(*d*); 20.6%] and S···H/H···S [Fig. 7(*e*); 9.0%] interactions have the greatest contributions to the surface contacts. The crystal packing is additionally influenced by C···C (2.2%), O···O (0.4%), O···C/C···O (0.3%), N···C/C···C (0.2%), S···C/C···S (0.1%) and S···O/O···S (0.1%) interactions. The large number of H···H, C···H/H···C, O···H/H···O and S···H/H···S interactions indicates that van der Waals interactions and hydrogen bonding are important in the crystal packing (Hathwar *et al.*, 2015).

4. Database survey

A search of the Cambridge Structural Database (CSD, Version 5.43, last update November 2022; Groom *et al.*, 2016) for the 1-benzothiophene unit yielded three compounds related to the title compound, *viz.* CSD refcode WOJBII (Kaur *et al.*, 2014), GAPZOO (Inaç *et al.*, 2012) and EYISEK (Sonar *et al.*, 2004).

In WOJBII, an intramolecular N—H···O hydrogen bond generates an $S(6)$ ring. In the crystal, very weak aromatic π–π stacking interactions [centroid–centroid separation = 3.9009 (10) Å] are observed. In GAPZOO, the molecular conformation features a short C—H···N contact. There are no significant intermolecular contacts. In EYISEK, intermolecular hydrogen bonding exists between the imino H atom and the Cl atoms, and gives rise to chains of molecules extending in the *c* direction. Van der Waals forces contribute to the stabilization of the crystal structure.

5. Synthesis and crystallization

Maleic anhydride (0.12 g, 1.3 mmol) was added to a solution of the corresponding allylamine **1** (0.37 g, 1.2 mmol) in benzene (10 ml). The resulting mixture was stirred for 6 h at room temperature. The resulting precipitate was filtered off, washed with benzene (5 ml), diethyl ether (2 × 5 ml) and air dried to give acid **3** (0.27 g, 74%) as a colourless solid (for full characterstics, see Yakovleva *et al.*, 2024). The mother liquor was mixed with C_2H_5OH (5 ml) and the precipitate was filtered off, washed with benzene (5 ml), diethyl ether (2 × 5 ml) and air dried to give the title compound **2** as a colourless powder (yield 18%, 0.09 g; m.p. 400–402 K). IR (KBr), ν (cm^{-1}): 3032 (OH), 1734 (CO_2), 1669 (N—C=O). ^{1}H NMR (600.2 MHz, DMSO-d_6, 298 K): δ (*J*, Hz) 12.71 (*s*, 1H, CO_2H), 7.93 (*d*, *J* = 8.1, 1H, H-Ar), 7.35–7.09 (*m*, 8H, H-Ar), 6.84 (*s*, 1H, H-2 benzothiophene), 6.37 (*d*, *J* = 12.1, 1H, H-2 CH=CH), 5.71 (*d*, *J* = 12.1, 1H, H-2 CH=CH), 4.36 (*br s*, 2H, NCH_2), 2.66–2.62 (*m*, 4H, H-3, H-5), 1.93 (*pent*, *J* = 7.6, 2H, H-4). ^{13}C {^{1}H} NMR (150.9 MHz, DMSO-d_6, 298 K): δ 166.0, 162.0, 140.4, 139.1, 138.5, 136.2, 135.2, 133.3, 132.1, 128.9 (2C), 128.0, 124.4, 124.3, 123.2, 122.8, 122.2, 119.0, 118.0 (2C), 52.9, 34.0, 31.7, 21.1. MS (ESI) *m/z*: [*M* + H]$^+$ 404. Elemental analysis calculated (%) for $C_{24}H_{21}NO_3S$: C 71.44, H 5.25, N 3.47, S 7.95; found: C 71.40, H 5.35, N 3.55, S, 7.91.

6. Refinement

Crystal data, data collection and structure refinement details are summarized in Table 2. All C-bound H atoms were positioned geometrically (C—H = 0.93 and 0.97 Å) and refined using a riding model with $U_{iso}(H) = 1.2U_{eq}(C)$. The O-bound H atom was located in difference Fourier maps [O29—H29 = 0.93 (4) Å] and refined freely.

Table 2
Experimental details.

Crystal data	
Chemical formula	$C_{24}H_{21}NO_3S$
M_r	403.48
Crystal system, space group	Triclinic, $P\bar{1}$
Temperature (K)	296
a, b, c (Å)	9.4270 (5), 9.4386 (4), 12.3849 (7)
α, β, γ (°)	95.392 (3), 96.849 (3), 106.512 (3)
V (Å^3)	1039.49 (9)
Z	2
Radiation type	Mo $K\alpha$
μ (mm^{-1})	0.18
Crystal size (mm)	$0.32 \times 0.26 \times 0.22$
Data collection	
Diffractometer	Bruker Kappa APEXII area-detector
Absorption correction	Multi-scan (*SADABS*; Bruker, 2008)
T_{min}, T_{max}	0.882, 0.961
No. of measured, independent and observed [$I > 2\sigma(I)$] reflections	13624, 4758, 2579
R_{int}	0.046
$(\sin \theta/\lambda)_{max}$ (Å^{-1})	0.650
Refinement	
$R[F^2 > 2\sigma(F^2)]$, $wR(F^2)$, S	0.049, 0.115, 0.99
No. of reflections	4758
No. of parameters	266
H-atom treatment	H atoms treated by a mixture of independent and constrained refinement
$\Delta\rho_{max}, \Delta\rho_{min}$ (e Å^{-3})	0.21, −0.24

Computer programs: *APEX4* and *SAINT* (Bruker, 2018), *SHELXT* (Sheldrick, 2015*a*), *SHELXL2018* (Sheldrick, 2015*b*), *ORTEP-3 for Windows* (Farrugia, 2012) and *PLATON* (Spek, 2020).

References

Abdelhamid, A. A., Mohamed, S. K., Khalilov, A. N., Gurbanov, A. V. & Ng, S. W. (2011). *Acta Cryst.* E**67**, o744.

Akbari Afkhami, F., Mahmoudi, G., Gurbanov, A. V., Zubkov, F. I., Qu, F., Gupta, A. & Safin, D. A. (2017). *Dalton Trans.* **46**, 14888–14896.

Aliyeva, V. A., Gurbanov, A. V., Guedes da Silva, M. F. C., Gomila, R. M., Frontera, A., Mahmudov, K. T. & Pombeiro, A. J. L. (2024). *Cryst. Growth Des.* **24**, 781–791.

Bernstein, J., Davis, R. E., Shimoni, L. & Chang, N.-L. (1995). *Angew. Chem. Int. Ed. Engl.* **34**, 1555–1573.

Bruker (2008). *SADABS*. Bruker AXS Inc., Madison, Wisconsin, USA.

Bruker (2018). *APEX4* and *SAINT*. Bruker AXS Inc., Madison, Wisconsin, USA.

Cremer, D. & Pople, J. A. (1975). *J. Am. Chem. Soc.* **97**, 1354–1358.

Farrugia, L. J. (2012). *J. Appl. Cryst.* **45**, 849–854.

Groom, C. R., Bruno, I. J., Lightfoot, M. P. & Ward, S. C. (2016). *Acta Cryst.* B**72**, 171–179.

Gurbanov, A. V., Kuznetsov, M. L., Karmakar, A., Aliyeva, V. A., Mahmudov, K. T. & Pombeiro, A. J. L. (2022*a*). *Dalton Trans.* **51**, 1019–1031.

Gurbanov, A. V., Kuznetsov, M. L., Mahmudov, K. T., Pombeiro, A. J. L. & Resnati, G. (2020). *Chem. A Eur. J.* **26**, 14833–14837.

Gurbanov, A. V., Kuznetsov, M. L., Resnati, G., Mahmudov, K. T. & Pombeiro, A. J. L. (2022*b*). *Cryst. Growth Des.* **22**, 3932–3940.

Gurbanov, A. V., Maharramov, A. M., Zubkov, F. I., Saifutdinov, A. M. & Guseinov, F. I. (2018). *Aust. J. Chem.* **71**, 190–194.

Hathwar, V. R., Sist, M., Jørgensen, M. R. V., Mamakhel, A. H., Wang, X., Hoffmann, C. M., Sugimoto, K., Overgaard, J. & Iversen, B. B. (2015). *IUCrJ*, **2**, 563–574.

Horak, Y. I., Lytvyn, R. Z., Homza, Y. V., Zaytsev, V. P., Mertsalov, D. F., Babkina, M. N., Nikitina, E. V., Lis, T., Kinzhybalo, V., Matiychuk, V. S., Zubkov, F. I., Varlamov, A. V. & Obushak, M. D. (2015). *Tetrahedron Lett.* **56**, 4499–4501.

Horak, Y. I., Lytvyn, R. Z., Laba, Y. V., Homza, Y. V., Zaytsev, V. P., Nadirova, M. A., Nikanorova, T. V., Zubkov, F. I., Varlamov, A. V. & Obushak, M. D. (2017). *Tetrahedron Lett.* **58**, 4103–4106.

Inaç, H., Dege, N., Gümüş, S., Ağar, E. & Soylu, M. S. (2012). *Acta Cryst.* E**68**, o361.

Kaur, M., Jasinski, J. P., Yathirajan, H. S., Yamuna, T. S. & Byrappa, K. (2014). *Acta Cryst.* E**70**, o951–o952.

Khalilov, A. N., Tüzün, B., Taslimi, P., Tas, A., Tuncbilek, Z. & Cakmak, N. K. (2021). *J. Mol. Liq.* **344**, 117761.

Kopylovich, M. N., Karabach, Y. Y., Mahmudov, K. T., Haukka, M., Kirillov, A. M., Figiel, P. J. & Pombeiro, A. J. L. (2011*a*). *Cryst. Growth Des.* **11**, 4247–4252.

Kopylovich, M. N., Mahmudov, K. T., Guedes da Silva, M. F. C., Martins, L. M. D. R. S., Kuznetsov, M. L., Silva, T. F. S., Fraústo da Silva, J. J. R. & Pombeiro, A. J. L. (2011*b*). *J. Phys. Org. Chem.* **24**, 764–773.

Kopylovich, M. N., Mahmudov, K. T., Haukka, M., Luzyanin, K. V. & Pombeiro, A. J. L. (2011*c*). *Inorg. Chim. Acta*, **374**, 175–180.

Krishna, G., Grudinin, D. G., Nikitina, E. V. & Zubkov, F. I. (2022). *Synthesis*, **54**, 797–863.

Mahmoudi, G., Dey, L., Chowdhury, H., Bauzá, A., Ghosh, B. K., Kirillov, A. M., Seth, S. K., Gurbanov, A. V. & Frontera, A. (2017*a*). *Inorg. Chim. Acta*, **461**, 192–205.

Mahmoudi, G., Khandar, A. A., Afkhami, F. A., Miroslaw, B., Gurbanov, A. V., Zubkov, F. I., Kennedy, A., Franconetti, A. & Frontera, A. (2019). *CrystEngComm*, **21**, 108–117.

Mahmoudi, G., Zangrando, E., Miroslaw, B., Gurbanov, A. V., Babashkina, M. G., Frontera, A. & Safin, D. A. (2021). *Inorg. Chim. Acta*, **519**, 120279.

Mahmoudi, G., Zaręba, J. K., Gurbanov, A. V., Bauzá, A., Zubkov, F. I., Kubicki, M., Stilinović, V., Kinzhybalo, V. & Frontera, A. (2017*b*). *Eur. J. Inorg. Chem.* **2017**, 4763–4772.

Mahmudov, K. T., Huseynov, F. E., Aliyeva, V. A., Guedes da Silva, M. F. C. & Pombeiro, A. J. L. (2021). *Chem. A Eur. J.* **27**, 14370–14389.

Mahmudov, K. T., Kopylovich, M. N., Haukka, M., Mahmudova, G. S., Esmaeila, E. F., Chyragov, F. M. & Pombeiro, A. J. L. (2013). *J. Mol. Struct.* **1048**, 108–112.

Nadirova, M. A., Laba, Y. V., Zaytsev, V. P., Sokolova, J. S., Pokazeev, K. M., Anokhina, V. A., Khrustalev, V. N., Horak, Y. I., Lytvyn, R. Z., Siczek, M., Kinzhybalo, V., Zubavichus, Y. V., Kuznetsov, M. L., Obushak, M. D. & Zubkov, F. I. (2020). *Synthesis*, **52**, 2196–2223.

Safavora, A. S., Brito, I., Cisterna, J., Cárdenas, A., Huseynov, E. Z., Khalilov, A. N., Naghiyev, F. N., Askerov, R. K. & Maharramov, A. M. (2019). *Z. Kristallogr. New Cryst. Struct.* **234**, 1183–1185.

Sheldrick, G. M. (2015*a*). *Acta Cryst.* A**71**, 3–8.

Sheldrick, G. M. (2015*b*). *Acta Cryst.* C**71**, 3–8.

Sonar, V. N., Parkin, S. & Crooks, P. A. (2004). *Acta Cryst.* C**60**, o550–o551.

Spackman, P. R., Turner, M. J., McKinnon, J. J., Wolff, S. K., Grimwood, D. J., Jayatilaka, D. & Spackman, M. A. (2021). *J. Appl. Cryst.* **54**, 1006–1011.

Spek, A. L. (2020). *Acta Cryst.* E**76**, 1–11.

research communications

Yakovleva, E. D., Shelukho, E. R., Nadirova, M. A., Erokhin, P. P., Simakova, D. N., Khrustalev, V. N., Grigoriev, M. S., Novikov, A. P., Romanycheva, A. A., Shetnev, A. A., Bychkova, O. P., Trenin, A. S., Zubkov, F. I. & Zaytsev, V. P. (2024). *Org. Biomol. Chem.* **22**, 2643–2653.

Zubkov, F. I., Zaytsev, V. P., Mertsalov, D. F., Nikitina, E. V., Horak, Y. I., Lytvyn, R. Z., Homza, Y. V., Obushak, M. D., Dorovatovskii, P. V., Khrustalev, V. N. & Varlamov, A. V. (2016). *Tetrahedron*, **72**, 2239–2253.

supporting information

Crystal structure and Hirshfeld surface analysis of (*Z*)-4-({[2-(benzo[*b*]thiophen-3-yl)cyclopent-1-en-1-yl]methyl}(phenyl)amino)-4-oxobut-2-enoic acid

Elizaveta D. Yakovleva, Evgeniya R. Shelukho, Mikhail S. Grigoriev, Khudayar I. Hasanov, Nurlana D. Sadikhova, Mehmet Akkurt and Ajaya Bhattarai

Computing details

(*Z*)-4-({[2-(Benzo[*b*]thiophen-3-yl)cyclopent-1-en-1-yl]methyl}(phenyl)amino)-4-oxobut-2-enoic acid

Crystal data

$C_{24}H_{21}NO_3S$	$Z = 2$
$M_r = 403.48$	$F(000) = 424$
Triclinic, $P\overline{1}$	$D_x = 1.289$ Mg m^{-3}
$a = 9.4270$ (5) Å	Mo $K\alpha$ radiation, $\lambda = 0.71073$ Å
$b = 9.4386$ (4) Å	Cell parameters from 2139 reflections
$c = 12.3849$ (7) Å	$\theta = 2.7–21.1°$
$\alpha = 95.392$ (3)°	$\mu = 0.18$ mm^{-1}
$\beta = 96.849$ (3)°	$T = 296$ K
$\gamma = 106.512$ (3)°	Fragment, colourless
$V = 1039.49$ (9) Å^3	$0.32 \times 0.26 \times 0.22$ mm

Data collection

Bruker Kappa APEXII area-detector diffractometer	4758 independent reflections
	2579 reflections with $I > 2\sigma(I)$
φ and ω scans	$R_{int} = 0.046$
Absorption correction: multi-scan (SADABS; Bruker, 2008)	$\theta_{max} = 27.5°$, $\theta_{min} = 4.3°$
	$h = -12 \rightarrow 12$
$T_{min} = 0.882$, $T_{max} = 0.961$	$k = -12 \rightarrow 12$
13624 measured reflections	$l = -16 \rightarrow 16$

Refinement

Refinement on F^2	Hydrogen site location: mixed
Least-squares matrix: full	H atoms treated by a mixture of independent and constrained refinement
$R[F^2 > 2\sigma(F^2)] = 0.049$	
$wR(F^2) = 0.115$	$w = 1/[\sigma^2(F_o^2) + (0.0397P)^2 + 0.1315P]$
$S = 0.99$	where $P = (F_o^2 + 2F_c^2)/3$
4758 reflections	$(\Delta/\sigma)_{max} < 0.001$
266 parameters	$\Delta\rho_{max} = 0.21$ e Å^{-3}
0 restraints	$\Delta\rho_{min} = -0.24$ e Å^{-3}

Special details

Geometry. All esds (except the esd in the dihedral angle between two l.s. planes) are estimated using the full covariance matrix. The cell esds are taken into account individually in the estimation of esds in distances, angles and torsion angles; correlations between esds in cell parameters are only used when they are defined by crystal symmetry. An approximate (isotropic) treatment of cell esds is used for estimating esds involving l.s. planes.

Fractional atomic coordinates and isotropic or equivalent isotropic displacement parameters (Å²)

	x	y	z	U_{iso}*/U_{eq}
S1	0.87037 (7)	0.68170 (6)	0.61573 (5)	0.0594 (2)
O21	0.1824 (3)	−0.0483 (2)	−0.14619 (18)	0.1267 (9)
O28	0.3378 (2)	0.04844 (18)	0.20444 (14)	0.0791 (6)
O29	0.1793 (3)	−0.0840 (2)	0.0262 (2)	0.1150 (9)
H29	0.224 (5)	−0.045 (4)	0.098 (3)	0.158 (16)*
N5	0.51977 (19)	0.26204 (18)	0.26864 (14)	0.0485 (5)
C1	0.5116 (2)	0.2342 (2)	0.38357 (17)	0.0521 (6)
H1A	0.415584	0.163072	0.386915	0.063*
H1B	0.517549	0.326562	0.428083	0.063*
C2	0.8233 (2)	0.5180 (2)	0.52668 (18)	0.0512 (6)
H2A	0.830032	0.515746	0.452274	0.061*
C3A	0.7750 (2)	0.4286 (2)	0.68961 (17)	0.0406 (5)
C3	0.7756 (2)	0.3932 (2)	0.57416 (17)	0.0424 (5)
C4	0.7341 (2)	0.3332 (2)	0.76803 (19)	0.0500 (6)
H4A	0.699452	0.230472	0.747835	0.060*
C5	0.7460 (3)	0.3934 (3)	0.8750 (2)	0.0671 (7)
H5A	0.718992	0.330231	0.927272	0.080*
C6	0.7974 (3)	0.5468 (3)	0.9073 (2)	0.0763 (8)
H6A	0.805046	0.584341	0.980612	0.092*
C7A	0.8246 (2)	0.5832 (2)	0.72381 (18)	0.0466 (5)
C7	0.8367 (3)	0.6423 (3)	0.8327 (2)	0.0630 (7)
H7A	0.870953	0.744824	0.854184	0.076*
C11	0.6337 (2)	0.1755 (2)	0.43046 (17)	0.0436 (5)
C12	0.7407 (2)	0.2407 (2)	0.51466 (16)	0.0426 (5)
C13	0.8318 (3)	0.1381 (2)	0.54573 (19)	0.0552 (6)
H13A	0.806912	0.098031	0.612696	0.066*
H13B	0.938174	0.189892	0.555652	0.066*
C14	0.7866 (3)	0.0148 (2)	0.4478 (2)	0.0598 (6)
H14A	0.861755	0.031363	0.399435	0.072*
H14B	0.775219	−0.081812	0.472422	0.072*
C15	0.6382 (3)	0.0221 (2)	0.38884 (19)	0.0554 (6)
H15A	0.635418	0.009946	0.309899	0.066*
H15B	0.554836	−0.054219	0.407358	0.066*
C21	0.2336 (4)	−0.0081 (3)	−0.0502 (3)	0.0835 (9)
C22	0.3591 (3)	0.1295 (3)	−0.0208 (2)	0.0683 (7)
H22A	0.388556	0.174848	−0.081361	0.082*
C23	0.4395 (3)	0.2030 (3)	0.07372 (19)	0.0645 (7)
H23A	0.513533	0.290349	0.068407	0.077*
C24	0.4279 (3)	0.1656 (2)	0.18604 (19)	0.0556 (6)

C31	0.6267 (2)	0.3994 (2)	0.25315 (16)	0.0423 (5)
C32	0.7609 (3)	0.3991 (2)	0.22026 (18)	0.0520 (6)
H32A	0.784507	0.310332	0.207993	0.062*
C33	0.8601 (3)	0.5327 (3)	0.2057 (2)	0.0636 (7)
H33A	0.949957	0.533354	0.181491	0.076*
C34	0.8276 (3)	0.6634 (3)	0.2264 (2)	0.0708 (8)
H34A	0.895368	0.752805	0.216795	0.085*
C35	0.6957 (4)	0.6629 (3)	0.2613 (2)	0.0696 (8)
H35A	0.674317	0.752324	0.276532	0.083*
C36	0.5938 (3)	0.5303 (2)	0.2740 (2)	0.0593 (6)
H36A	0.503131	0.530002	0.296694	0.071*

Atomic displacement parameters (Å^2)

	U^{11}	U^{22}	U^{33}	U^{12}	U^{13}	U^{23}
S1	0.0715 (4)	0.0433 (3)	0.0593 (4)	0.0106 (3)	0.0078 (3)	0.0104 (3)
O21	0.177 (2)	0.0925 (15)	0.0651 (15)	−0.0041 (15)	−0.0275 (15)	−0.0161 (12)
O28	0.0936 (13)	0.0594 (10)	0.0586 (12)	−0.0113 (10)	−0.0108 (10)	0.0158 (9)
O29	0.155 (2)	0.0688 (13)	0.0749 (16)	−0.0215 (13)	−0.0289 (15)	0.0109 (12)
N5	0.0521 (11)	0.0506 (10)	0.0382 (11)	0.0113 (9)	−0.0011 (9)	0.0063 (8)
C1	0.0502 (14)	0.0593 (13)	0.0408 (14)	0.0087 (11)	0.0033 (11)	0.0057 (11)
C2	0.0588 (14)	0.0500 (12)	0.0416 (13)	0.0111 (11)	0.0064 (11)	0.0088 (10)
C3A	0.0347 (11)	0.0445 (11)	0.0423 (13)	0.0121 (9)	0.0037 (9)	0.0067 (9)
C3	0.0408 (12)	0.0462 (11)	0.0382 (13)	0.0111 (10)	0.0022 (10)	0.0069 (9)
C4	0.0525 (14)	0.0518 (12)	0.0486 (15)	0.0157 (11)	0.0138 (11)	0.0124 (11)
C5	0.0861 (19)	0.0754 (17)	0.0500 (17)	0.0312 (15)	0.0246 (14)	0.0196 (13)
C6	0.106 (2)	0.0870 (19)	0.0440 (16)	0.0427 (18)	0.0152 (15)	−0.0004 (14)
C7A	0.0470 (13)	0.0486 (12)	0.0440 (14)	0.0162 (10)	0.0031 (10)	0.0043 (10)
C7	0.0771 (18)	0.0578 (14)	0.0537 (17)	0.0250 (13)	0.0048 (14)	−0.0032 (13)
C11	0.0491 (13)	0.0439 (11)	0.0344 (12)	0.0075 (10)	0.0067 (10)	0.0075 (9)
C12	0.0490 (13)	0.0414 (10)	0.0356 (12)	0.0090 (10)	0.0088 (10)	0.0082 (9)
C13	0.0633 (15)	0.0535 (12)	0.0488 (15)	0.0192 (12)	0.0022 (12)	0.0097 (11)
C14	0.0716 (17)	0.0466 (12)	0.0604 (16)	0.0185 (12)	0.0070 (13)	0.0048 (11)
C15	0.0676 (16)	0.0461 (12)	0.0449 (14)	0.0082 (11)	0.0034 (12)	0.0025 (10)
C21	0.119 (3)	0.0541 (15)	0.060 (2)	0.0158 (16)	−0.0188 (19)	−0.0045 (15)
C22	0.091 (2)	0.0615 (15)	0.0466 (16)	0.0204 (14)	−0.0031 (14)	0.0054 (12)
C23	0.0765 (18)	0.0586 (14)	0.0455 (16)	0.0042 (13)	−0.0044 (13)	0.0097 (12)
C24	0.0632 (15)	0.0500 (13)	0.0474 (15)	0.0120 (12)	−0.0043 (12)	0.0070 (11)
C31	0.0476 (13)	0.0441 (11)	0.0350 (12)	0.0171 (10)	−0.0016 (10)	0.0041 (9)
C32	0.0549 (15)	0.0567 (13)	0.0479 (14)	0.0254 (12)	0.0006 (12)	0.0062 (11)
C33	0.0462 (14)	0.0824 (18)	0.0582 (17)	0.0130 (13)	0.0005 (12)	0.0180 (14)
C34	0.075 (2)	0.0585 (16)	0.0597 (18)	−0.0027 (14)	−0.0144 (15)	0.0168 (13)
C35	0.095 (2)	0.0478 (14)	0.0624 (18)	0.0272 (15)	−0.0095 (16)	0.0012 (12)
C36	0.0627 (15)	0.0587 (14)	0.0608 (16)	0.0286 (13)	0.0033 (13)	0.0051 (12)

Geometric parameters (Å, º)

S1—C2	1.725 (2)	C11—C15	1.505 (3)
S1—C7A	1.728 (2)	C12—C13	1.512 (3)
O21—C21	1.210 (3)	C13—C14	1.529 (3)
O28—C24	1.247 (3)	C13—H13A	0.9700
O29—C21	1.305 (4)	C13—H13B	0.9700
O29—H29	0.93 (4)	C14—C15	1.522 (3)
N5—C24	1.338 (3)	C14—H14A	0.9700
N5—C31	1.443 (3)	C14—H14B	0.9700
N5—C1	1.478 (3)	C15—H15A	0.9700
C1—C11	1.495 (3)	C15—H15B	0.9700
C1—H1A	0.9700	C21—C22	1.468 (4)
C1—H1B	0.9700	C22—C23	1.329 (3)
C2—C3	1.352 (3)	C22—H22A	0.9300
C2—H2A	0.9300	C23—C24	1.476 (3)
C3A—C4	1.399 (3)	C23—H23A	0.9300
C3A—C7A	1.406 (3)	C31—C36	1.367 (3)
C3A—C3	1.439 (3)	C31—C32	1.375 (3)
C3—C12	1.482 (3)	C32—C33	1.382 (3)
C4—C5	1.370 (3)	C32—H32A	0.9300
C4—H4A	0.9300	C33—C34	1.362 (3)
C5—C6	1.391 (3)	C33—H33A	0.9300
C5—H5A	0.9300	C34—C35	1.363 (4)
C6—C7	1.361 (4)	C34—H34A	0.9300
C6—H6A	0.9300	C35—C36	1.380 (4)
C7A—C7	1.389 (3)	C35—H35A	0.9300
C7—H7A	0.9300	C36—H36A	0.9300
C11—C12	1.326 (3)		
C2—S1—C7A	90.81 (10)	C14—C13—H13B	111.1
C21—O29—H29	116 (2)	H13A—C13—H13B	109.0
C24—N5—C31	123.48 (18)	C15—C14—C13	105.85 (18)
C24—N5—C1	120.39 (19)	C15—C14—H14A	110.6
C31—N5—C1	116.08 (16)	C13—C14—H14A	110.6
N5—C1—C11	112.78 (18)	C15—C14—H14B	110.6
N5—C1—H1A	109.0	C13—C14—H14B	110.6
C11—C1—H1A	109.0	H14A—C14—H14B	108.7
N5—C1—H1B	109.0	C11—C15—C14	103.55 (17)
C11—C1—H1B	109.0	C11—C15—H15A	111.1
H1A—C1—H1B	107.8	C14—C15—H15A	111.1
C3—C2—S1	114.34 (17)	C11—C15—H15B	111.1
C3—C2—H2A	122.8	C14—C15—H15B	111.1
S1—C2—H2A	122.8	H15A—C15—H15B	109.0
C4—C3A—C7A	118.37 (19)	O21—C21—O29	121.5 (3)
C4—C3A—C3	129.57 (19)	O21—C21—C22	118.3 (3)
C7A—C3A—C3	112.06 (18)	O29—C21—C22	120.2 (2)
C2—C3—C3A	111.32 (18)	C23—C22—C21	133.7 (3)

C2—C3—C12	123.2 (2)	C23—C22—H22A	113.2
C3A—C3—C12	125.29 (18)	C21—C22—H22A	113.2
C5—C4—C3A	119.1 (2)	C22—C23—C24	129.1 (2)
C5—C4—H4A	120.5	C22—C23—H23A	115.5
C3A—C4—H4A	120.5	C24—C23—H23A	115.5
C4—C5—C6	121.6 (2)	O28—C24—N5	120.6 (2)
C4—C5—H5A	119.2	O28—C24—C23	122.1 (2)
C6—C5—H5A	119.2	N5—C24—C23	117.3 (2)
C7—C6—C5	120.7 (2)	C36—C31—C32	120.5 (2)
C7—C6—H6A	119.7	C36—C31—N5	118.8 (2)
C5—C6—H6A	119.7	C32—C31—N5	120.68 (18)
C7—C7A—C3A	121.8 (2)	C31—C32—C33	119.0 (2)
C7—C7A—S1	126.71 (17)	C31—C32—H32A	120.5
C3A—C7A—S1	111.46 (16)	C33—C32—H32A	120.5
C6—C7—C7A	118.5 (2)	C34—C33—C32	120.6 (2)
C6—C7—H7A	120.8	C34—C33—H33A	119.7
C7A—C7—H7A	120.8	C32—C33—H33A	119.7
C12—C11—C1	126.95 (18)	C33—C34—C35	119.9 (2)
C12—C11—C15	112.06 (18)	C33—C34—H34A	120.1
C1—C11—C15	120.81 (18)	C35—C34—H34A	120.1
C11—C12—C3	127.71 (18)	C34—C35—C36	120.3 (2)
C11—C12—C13	111.02 (17)	C34—C35—H35A	119.8
C3—C12—C13	121.27 (17)	C36—C35—H35A	119.8
C12—C13—C14	103.43 (17)	C31—C36—C35	119.6 (2)
C12—C13—H13A	111.1	C31—C36—H36A	120.2
C14—C13—H13A	111.1	C35—C36—H36A	120.2
C12—C13—H13B	111.1		
C24—N5—C1—C11	102.2 (2)	C2—C3—C12—C13	115.1 (2)
C31—N5—C1—C11	−80.0 (2)	C3A—C3—C12—C13	−59.9 (3)
C7A—S1—C2—C3	−0.32 (18)	C11—C12—C13—C14	13.8 (3)
S1—C2—C3—C3A	0.4 (2)	C3—C12—C13—C14	−165.47 (19)
S1—C2—C3—C12	−175.16 (15)	C12—C13—C14—C15	−19.8 (2)
C4—C3A—C3—C2	−179.9 (2)	C12—C11—C15—C14	−10.9 (3)
C7A—C3A—C3—C2	−0.4 (2)	C1—C11—C15—C14	173.7 (2)
C4—C3A—C3—C12	−4.4 (3)	C13—C14—C15—C11	18.7 (2)
C7A—C3A—C3—C12	175.13 (19)	O21—C21—C22—C23	−179.9 (3)
C7A—C3A—C4—C5	−0.9 (3)	O29—C21—C22—C23	0.3 (5)
C3—C3A—C4—C5	178.6 (2)	C21—C22—C23—C24	0.9 (5)
C3A—C4—C5—C6	0.1 (4)	C31—N5—C24—O28	179.9 (2)
C4—C5—C6—C7	0.5 (4)	C1—N5—C24—O28	−2.5 (3)
C4—C3A—C7A—C7	1.3 (3)	C31—N5—C24—C23	0.6 (3)
C3—C3A—C7A—C7	−178.3 (2)	C1—N5—C24—C23	178.22 (19)
C4—C3A—C7A—S1	179.73 (15)	C22—C23—C24—O28	3.1 (4)
C3—C3A—C7A—S1	0.1 (2)	C22—C23—C24—N5	−177.6 (2)
C2—S1—C7A—C7	178.4 (2)	C24—N5—C31—C36	102.1 (2)
C2—S1—C7A—C3A	0.09 (16)	C1—N5—C31—C36	−75.6 (2)
C5—C6—C7—C7A	−0.1 (4)	C24—N5—C31—C32	−79.3 (3)

C3A—C7A—C7—C6	−0.8 (3)	C1—N5—C31—C32	103.1 (2)
S1—C7A—C7—C6	−178.9 (2)	C36—C31—C32—C33	−1.8 (3)
N5—C1—C11—C12	117.2 (2)	N5—C31—C32—C33	179.64 (19)
N5—C1—C11—C15	−68.1 (3)	C31—C32—C33—C34	1.8 (3)
C1—C11—C12—C3	−7.6 (4)	C32—C33—C34—C35	−0.4 (4)
C15—C11—C12—C3	177.3 (2)	C33—C34—C35—C36	−1.0 (4)
C1—C11—C12—C13	173.2 (2)	C32—C31—C36—C35	0.4 (3)
C15—C11—C12—C13	−1.9 (3)	N5—C31—C36—C35	179.0 (2)
C2—C3—C12—C11	−64.0 (3)	C34—C35—C36—C31	1.0 (4)
C3A—C3—C12—C11	121.0 (2)		

Hydrogen-bond geometry (Å, º)

*Cg*3 and *Cg*4 are the centroids of the benzene ring (C3A/C4–C7/C7A) of the nine-membered ring system (S1/C2-C3/C3A/C4–C7/C7A) and the phenyl ring (C31–C36), respectively.

D—H···*A*	*D*—H	H···*A*	*D*···*A*	*D*—H···*A*
O29—H29···O28	0.93 (4)	1.60 (4)	2.510 (3)	164 (4)
C32—H32*A*···O21[i]	0.93	2.63	3.556 (3)	171
C2—H2*A*···*Cg*4	0.93	2.72	3.579 (2)	154
C33—H33*A*···*Cg*3[ii]	0.93	2.54	3.408 (3)	155
C33—H33*A*···*Cg*5[ii]	0.93	2.64	3.353 (3)	133
C36—H36*A*···*Cg*3[iii]	0.93	2.79	3.535 (3)	138
C36—H36*A*···*Cg*5[iii]	0.93	2.75	3.623 (3)	157

Symmetry codes: (i) −*x*+1, −*y*, −*z*; (ii) −*x*+2, −*y*+1, −*z*+1; (iii) −*x*+1, −*y*+1, −*z*+1.